Journal of Applied Biology & Biotechnology Vol. 11(6), pp. 178-184, Nov-Dec, 2023
Available online at http://www.jabonline.in
DOI: 10.7324/JABB.2023.131095

In vitro antioxidant and acetylcholinesterase activities of catechin-loaded green fabricated zinc oxide nanoparticles

Nandhini Baskaran, Anitha Subash*

Department of Biochemistry, Biotechnology, and Bioinformatics, Avinashilingam Institute for Home Science and Higher Education for Women, Coimbatore, Tamil Nadu, India.

ARTICLE INFO

Article history:
Received on: March 21, 2023
Accepted on: July 04, 2023
Available online: October 25, 2023

Key words:
Acetylcholinesterase,
Catechin, Catechin-coated zinc oxide nanoparticles,
Neuroprotective activity.

ABSTRACT

Catechin is an antioxidant, secondary metabolite found in *Camellia sinensis* that has unique qualities such as antioxidant activity, acetylcholinesterase activity, and neuroprotective benefit. In addition to having poor biological efficacy due to low stability, nanotechnology can enhance or improve stability. The aim of this study is to synthesize catechin-coated zinc oxide nanoparticles (CAT-ZnONPs) using *C. sinensis* leaf extract by the nanoprecipitation method and investigate their *in vitro* antioxidant and acetylcholinesterase activities. The ultraviolet-visible spectrophotometer and the Fourier transform infrared spectrophotometer were used to characterize the CAT-ZnONPs; the particle had a consistent distribution and no agglomeration of nanoparticles was observed using field emission-scanning electron microscopy. Based on X-ray diffraction (XRD) analysis, the average size of CAT-ZnONPs is between 50 and 60 nm, as measured using the intensity of XRD. *In vitro,* the antioxidant activity of CAT-ZnONPs using the DPPH technique showed 50% scavenging at a dosage of 35 µg/mL. *In vitro* acetylcholinesterase inhibition activity of CAT-ZnONPs with a IC_{50} concentration of 1.25 µg/mL was demonstrated. Thus, the obtained results revealed the first study to demonstrate CAT-ZnONPs as a therapeutic agent, which could be a promising drug delivery system and provide a novel process for curative intervention in neurological disorders in future research.

1. INTRODUCTION

Nanotechnology is a branch of interdisciplinary research that attracts researchers from many fields, including medicine, electronics, and biomaterials. Nanomaterials can be made with dimensions as small as 10–100 nm by a variety of methods, such as biological, chemical, and physical [1]. Nanotechnology is used in a wide variety of fields. In the food industry, nanocomposites are used to determine the amount of tartrazine (TRT) in food samples, and some carbon nanotubes (CNT), graphene (GR) are used in an electrochemical sensing system to detect the azo dye contaminations in food samples [2,3]. In biomedical applications, nanoparticles have a significant role in cancer therapy through targeted drug delivery and provide new approaches for diagnosis and biosensing [4]. In the biosensor application used to detect glutathione in body fluids, glutathione is used as an antioxidant to prevent the cells from oxidative damage caused by free radicals [5]. In environmental remediation photocatalytic application, nanocomposite is a good photocatalyst for degrading the organic compound nitrobenzene under light irradiation [6]. In waste water treatment, nanocomposite significantly improves its adsorption character for the deduction of metal ions, pharmaceutical waste, pesticides, organic pollutants, and heavy metals [7,8]. Nanomaterials have attracted the attention of scientists due to their unique properties, such as their high surface area, small size, thermal conductivity, shape, surface morphology, charge, zeta potential, and crystal structure [9]. These properties have led to their incorporation into the biotechnological and biomedical fields, especially in the treatment of fatal diseases such as cancer and Alzheimer's [10,11]. The green synthesis is a preferred method for nanoparticle synthesis due to its low cost, environmental friendliness, biocompatibility, ease of use, and rapid synthesis methods [12]. Different kinds of organisms, such as cyanobacteria, fungi, actinomycetes, bacteria, algae, and plants, are capable of synthesizing nanoparticles. Green synthesis has allowed for the synthesis of a wide variety of nanoparticles with diverse biological activities, including silver, copper, gold, zinc oxide, selenium oxide, and copper oxide [13-16]. Zinc is a vital mineral and an essential component for human development. Zinc deficiency can result in a wide variety of symptoms, including growth retardation, premature death, and problems with both male and female reproduction. ZnO-NPs are used in cosmetics and sunscreens because of their powerful ultraviolet (UV) absorption characteristics [17]. In addition to investigating their *in vitro* cytotoxic ability against cancer cells, researchers also tested ZnO-NPs for their potential to treat Alzheimer's disease and diabetes [18].

The plant *Camellia sinensis,* from the family Theaceae, is used to make the green, black, that are so popular around the world. However, green tea consumption has been shown to have the most dramatic effects on

*Corresponding Author:
Dr. Anitha Subash, Department of Biochemistry, Biotechnology, and Bioinformatics, Avinashilingam Institute for Home Science and Higher Education for Women, Coimbatore, Tamil Nadu, India.
E-mail: dranithasubash @ gmail.com

human health [19]. Tea leaf production is widespread throughout the world, with the majority consumed in Asia, some regions of North Africa, the United States, and Europe [20]. Catechins, flavanols, flavanones, phenolic acids, glycosides, and aglycones of plant pigments are just some of the phytochemicals found in *C. sinensis* [21]. Catechins have excellent antioxidant properties and are found in abundance in fresh tea leaves; they can account for up to 30% of the dry weight of the leaves [19]. The anti-cancer, anti-heart disease, anti-Alzheimer's, and anti-aging properties of *C. sinensis* are well documented [22]. The phenolic compounds served as a good reducing agent to reduce metal ions for the green synthesis of nanoparticles and had a stronger antioxidant capacity than other types of phytochemicals. *C. sinensis* have more consisted of proteins, lipids, and amino acids which is the influence to nanoparticle growth and reduced agglomeration [23].

This study will focus on the synthesis of zinc oxide nanoparticles (CAT-ZnONPs) using *C. sinensis* leaf extract and coated with catechine, which is enhance the bioactive potential and promise as antioxidants and acetylcholinesterase inhibitors. Analytical characterization of the green-synthesized CAT-ZnONPs using various techniques such as–visible spectrum analysis, scanning electron microscopy (SEM) with energy dispersive X-ray spectroscopy (EDAX), elemental mapping, Fourier transform infrared spectroscopy (FTIR), and X-ray diffraction (XRD). All the above characterizations are used to analyze the nanoparticle's topography, morphology, composition, and crystalline structure.

2. MATERIALS AND METHODS

2.1. Materials

Zinc acetate dihydrate $Zn(CH_3COO)_2.2H_2O$, Catechin and Ellman assay kit for AChE activity were procured from Sigma-Aldrich Chemical, Coimbatore and all Other Chemicals procured from HiMedia and were of analytical quality.

2.2. Synthesis of ZnONPs

According to Gnanasangeetha and Thambavani [24], the biosynthesis method was used to synthesize zinc oxide nanoparticles (ZnONPs) with some modifications. Zinc acetate dihydrate and sodium hydroxide were used as the precursors that were employed in the synthesis of nanoparticles. The 200 mM zinc acetate dihydrate solution was dissolved in 20 mL of distilled water and vigorously stirred in a magnetic stirrer. Following the addition of 5 mL aqueous extracts of *C. sinensis* leaf with zinc acetate solution, and then the addition of 2M of NaOH to make pH-12, the mixture was stirred in for 2 h at 60°C. Then, other elements were removed from the final precipitation using centrifugation at 1400 rpm for 5 min and washed with distilled water and ethanol. The precipitate was dried at 60°C overnight, then the dried white precipitate was powdered using an agate mortar, and the final ZnONPs were stored in an airtight container.

2.3. Preparation of CAT-ZnONPs

The catechin was coated on the surface of zinc oxide nanoparticles by the nanoprecipitation method with modifications according to Arasoğlu *et al.*, Liu *et al.* [25,26]. In a brief procedure, 100 mg of ZnONPs were dissolved in 5 mL of 0.01 N HCl and 10mg of CAT were dissolved in 5mL of ethanol with continuous stirring. 5 mL CAT solution was added drop by drop to the ZnONPs. During stirring, NaOH was added to the ZnONPs and CAT mixture for precipitate formation, and the pH was adjusted to 5.0. The obtained precipitate was centrifuged at 16,000 g at room temperature for 30 min, and the CAT-ZnONPs have been dried using freeze drying at −50°C for 24 h.

2.4. Characterization of CAT-ZnONPs

CAT-ZnONPs' Fourier transform-infrared spectra were captured by a Shimadzu Fourier-transform infrared (FT-IR) 8400 spectrophotometer in the 600–4000 cm^{-1} range, and UV–visible spectrum analysis was carried out using a Shimadzu 1800 spectrophotometer. Morphological identification of nanoparticles was analyzed by field emission FE-SEM, EDAX was used to analyze purification of nanoparticle and elements containing nanoparticles. An elemental mapping analysis was used to study the shape, structure, and composition of the CAT-ZnONPs. Particle size distribution and crystallinity of nanoparticles were analyzed using XRD.

2.5. DPPH radical scavenging activity of CAT-ZnONPs

CAT-ZnONPs's ability to scavenge the free radicals was investigated using the 2, 2-diphenyl-1-picrylhydrazile (DPPH) technique, as described in Rahman *et al.*, Najafabadand and Jamei [27,28] with some modifications. Different concentrations of CAT-ZnO NPs, from 25 µg/mL to 45 µg/mL were added to a 96-well plate containing a 1 mM DPPH solution. Ascorbic acid (Vitamin C) is used as the standard solution, followed by 30 min of incubation at room temperature in the dark. In methanol, DPPH appears purple but fades to yellow when neutralized by antioxidants. After incubation, the decolorization of DPPH may be observed, denoting the CAT-ZnONPs' ability to donate hydrogen atoms as antioxidants. The scavenging ability was measured at 517 nm absorbance. The experiment has been demonstrated in triplicate and calculated with a mean ± standard deviation. The scavenging capacity was estimated using the following equation:

$$\%\,\text{DPPH radical scavenging activity} = \frac{(A0\text{-}A1)}{A0} \times 100\%$$

Whereas, A0–OD value of blank, A1–OD value of Standard/CAT-ZnO NPs treated. The IC_{50} was calculated by a graph plotting the concentration of CAT-ZnO NPs against % of inhibition.

2.6. Thin-layer chromatography (TLC) with bioassay detection for AChE inhibition

The TLC with bioassay detection for AChE inhibition was altered from the study of Rhee *et al.* [29]. The stationary phase was a 25 mm F254 no. 5554 silica gel plate. Two mobile phases were used: dichloromethane: ethanol:water (4:4:0.5 v/v/v) and chloroform: methanol (9:1 v/v). On the plate, 3 µL of plant extracts in methanol were administered at a concentration of 5 mg/mL. Once the plate had been produced, it was allowed to dry at ambient temperature before being sprayed with 20 mM DTNB and 30 mM ATCI. The plate was dried at room temperature for 45 min before being sprayed with 10.17 U/mL AChE.

2.7. Acetylcholinesterase inhibition activity

The Ellman assay kit method was used to measure the acetylcholinesterase inhibition activity. A 96-well microtiter plate was filled to a volume of 100 L with assay buffer as a control without enzyme, and 100 L of AChE enzyme was added into the wells, followed by different concentrations of the nanoparticles with the enzyme: 0.25, 0.5, 0.75, 1.0, 1.25, 1.50, and 1.75 L. The plate was incubated for 5 min at room temperature. After that, 180 µL of Ellman's reagent was added to each well. The change has been observed in 412 nm absorbance. The experiment has been demonstrated in triplicate. The AChE activity was calculated as a percentage based on the formula.

$$\text{Enzyme activity } (\%) = \frac{E - S}{E} \times 100$$

Where E represents the AChE activity without a CAT-ZnONPs and S represents the enzyme's activity when a CAT-ZnONPs is present.

3. RESULTS AND DISCUSSION

3.1. UV-visible spectrum of (CAT-ZnONPs)

In the present study, we investigated the synthesis of zinc oxide nanoparticles coated with catachin (CAT-ZnONPs) using nanoprecipitation methods. Figure 1 shows the UV spectra of CAT-ZnONPs measured at 318 nm absorbance. The reaction stimulated for 1 h at a temperature of 26°C was fast and also used up minimal energy. In earlier research, we had established that catechin-AuNPs had been successfully synthesized [23].

3.2. FE-SEM and EDAX analyses of CAT-ZnONPs

FE-SEM is used to evaluate the surface morphology of the obtained CAT-ZnONPs, as shown in Figure 2. The distribution of nanoparticles has similar size and shape in the solution, which has the flower shape revealed by FE-SEM. The particle surface appeared to be smooth and agglomerated, which proves the catechin was coated on ZnONP. In the earlier study, quercetin-loaded PLGA nanoparticles were observed in FE-SEM images, and the hydrophobic properties of the morphological changes were investigated without the use of a solvent [24,30].

Only the peaks of the elements zinc, oxygen, chlorine, and potassium are found in the EDAX spectrum of CAT-ZnONPs, as shown in Figure 3. In the EDS limit, it is apparent that the ZnONPs prepared are completely free of impurities. According to the EDAX spectrum, Zn and O have very high atomic weights, and other components such as chlorine and potassium are present in very small amounts. As a result of the results, Zn and O were found in high concentrations in the nanoparticles, and the nanoparticles' high purity was demonstrated by the EDAX spectrum [Figure 3].

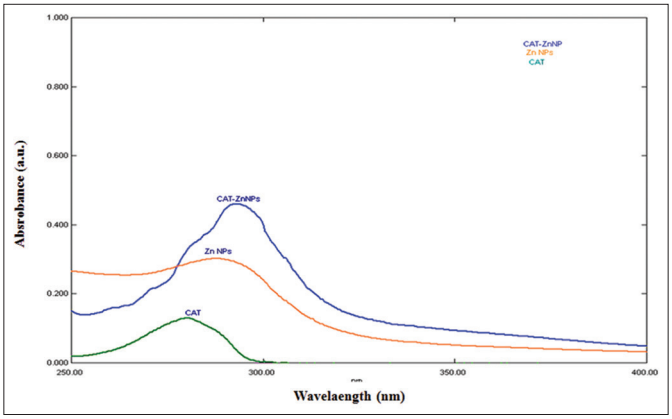

Figure 1: Ultraviolet-visible spectrum of catechin-coated zinc oxide nanoparticles.

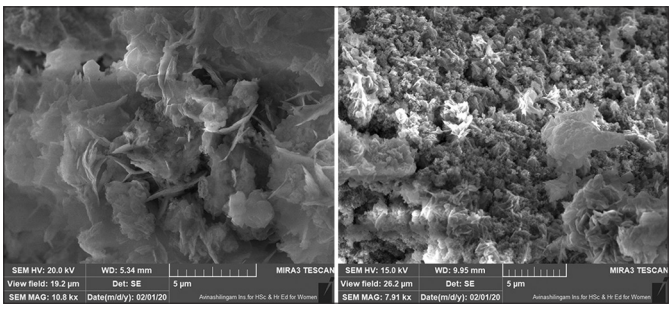

Figure 2: Field emission-scanning electron microscopy analysis of catechin-coated zinc oxide nanoparticles.

3.3. Elemental Mapping analysis of CAT-ZnONPs

To further support the EDAX spectrum's elemental investigation of CAT-ZnONPs. The elemental mapping only shows the zinc and oxygen peaks, as shown in Figure 4. These results showed a high signal from Zn atoms (75.03%) and O atoms (16.42% suggesting that catechin was successfully coated on the surface of ZnONPs. The visible peaks for other elements such as C atoms (8.13%) and K atoms (0.45%) were observed to be much lower. In a previous report, Tet-1 peptide successfully coated the surface of EGCG@Se, as shown by the elemental composition mapping study [31] which showed a strong single from Se along with C, N, and O atoms.

3.4. XRD patterns of CAT-ZnONPs

XRD spectroscopy confirmed the metallic Zn's crystalline structure in [Figure 5]. Peaks of intense diffraction were seen in the face-centered (100), (111), (101), (102), (110), (103), (112), (004), and (311) planes,

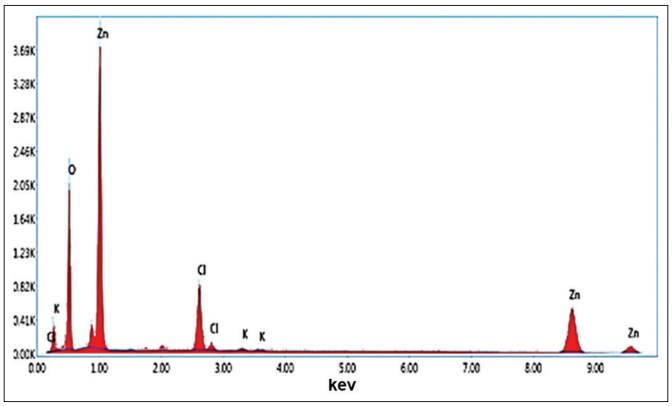

Figure 3: Energy dispersive X-ray spectroscopy spectrum of catechin-coated zinc oxide nanoparticles.

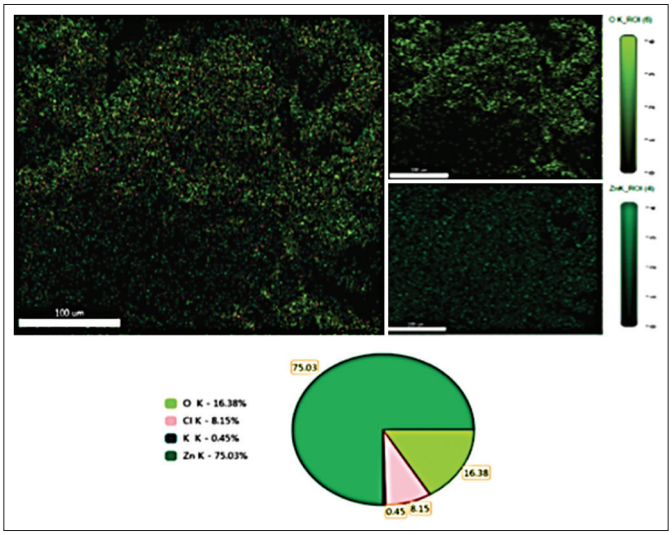

Figure 4: Elemental mapping analysis of catechin-coated zinc oxide nanoparticles.

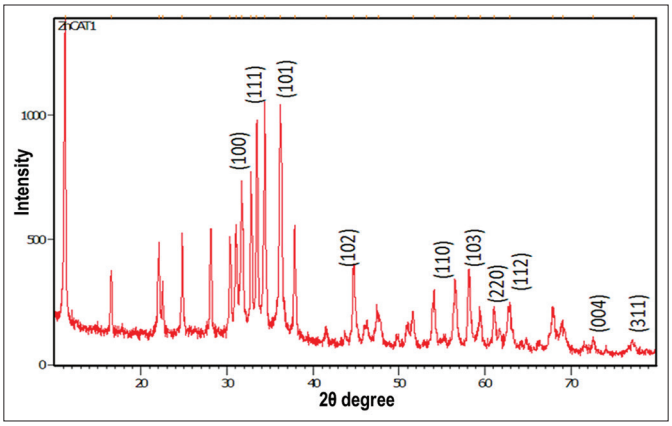

Figure 5: X-ray diffraction patterns of catechin-coated zinc oxide nanoparticles 2θ.

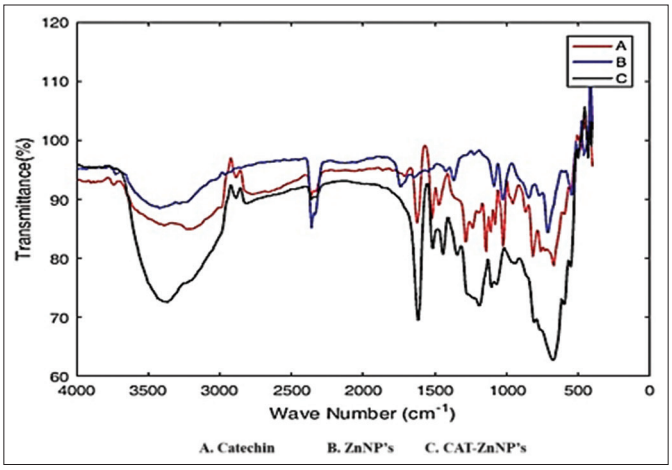

Figure 6: Fourier-transform infrared spectrum of catechin-coated zinc oxide nanoparticles.

respectively, at 31.9, 34.05, 36.02, 45.0, 56.86, 58.0, 61.0, 63.0, 72.28, and 77.7 (fcc). The strongest peak appeared at 34.05, indicating that the (111) plane was the most frequent orientation. Using the intensity of diffraction from Debye-Scherrer equation, the average size of CAT-ZnONPs is between 50 and 60 nm and was measured [32].

3.5. FT-IR spectrum of CAT-ZnONPs

FT-IR was used to further characterize CAT-ZnONPs to establish the existence of the chemical bonds depicted in Figure 6. The presence of the OH group was indicated by a broad, strong band in the FT-IR spectrum of the CAT-ZnONPs that ranged from 3446 cm^{-1}. 1620cm^{-1} peak responsible for the alkenyl C=C stretch. In addition, a weak band at 1442cm^{-1} was observed as a result of the methyl C-H bend vibration. A narrow band at 1519cm^{-1} is formed by the sample's -CO group and the fraction of catechin-coated zinc oxide nanoparticles. The band at 3387cm^{-1} is responsible for OH stretching strong bond As a result, the OH group's presence in the extract is confirmed. Zhang *et al.* [33] reported that the FT-IR spectrum of Tet-1 EGCC@Set was examined to investigate possible interactions to confirm the presence of Tet-1 on the surface of SeNPs.

3.6. Antioxidant activity of CAT-ZnONPs

Figure 7 depicts the DPPH scavenging activity of CAT-ZnONPs. The percentage inhibition of scavenging activity of CAT-ZnONPs was increasing in a dose-dependent manner that was comparable to that of standard ascorbic acid at the same concentration given as Supplementary Table1. The IC_{50} value of the CAT-ZnONPs was determined based on the 50% of free radicals scavenged by 35 µg/mL. Earlier, it was reported by Mathew *et al.* [34] that the attachment of Tet-1 to the curcumin-PLGA nanoparticles did not produce any change in their antioxidant activity. The point to be noted is that the CAT-ZnONPs do not destroy the antioxidant activity of catechin. Phenolic compounds and catechins found in *C. sinensis* is backbone of efficient antioxidant activity in the 96% of ethanolic extract has reported in past research [19]. In early reported antioxidant activity of *C. sinensis* extract with a concentration of IC_{50} 70.25 ± 2.85 µg/mL [22]

3.7. TLC qualitative acetylcholinesterase inhibition (AChEI) assay

An investigation of autographic assay using the TLC for qualitative examination of acetylcholinesterase inhibition (AChEI) [Figure 8].

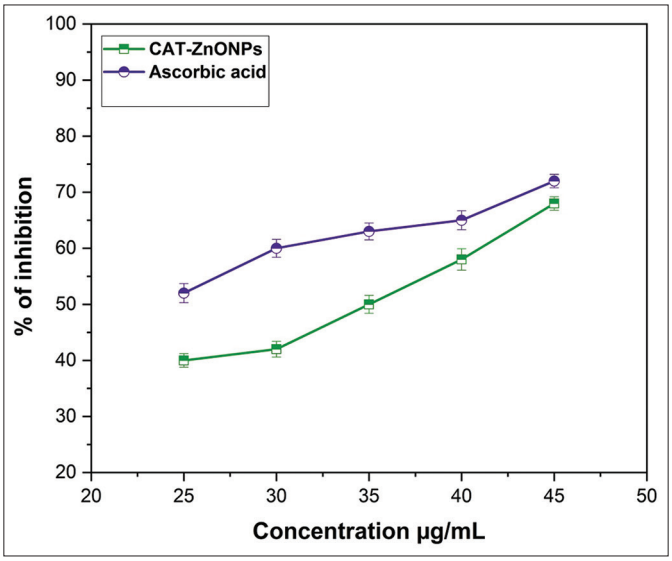

Figure 7: Antioxidant activity of catechin-coated zinc oxide nanoparticles.

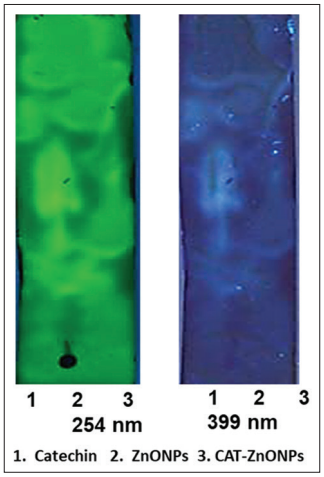

Figure 8: Acetylcholinesterase inhibition qualitative thin layer chromatography (TLC) assay, TLC elution system: Dichloromethane: Ethanol:water (4:4:0.5 v/v/v).

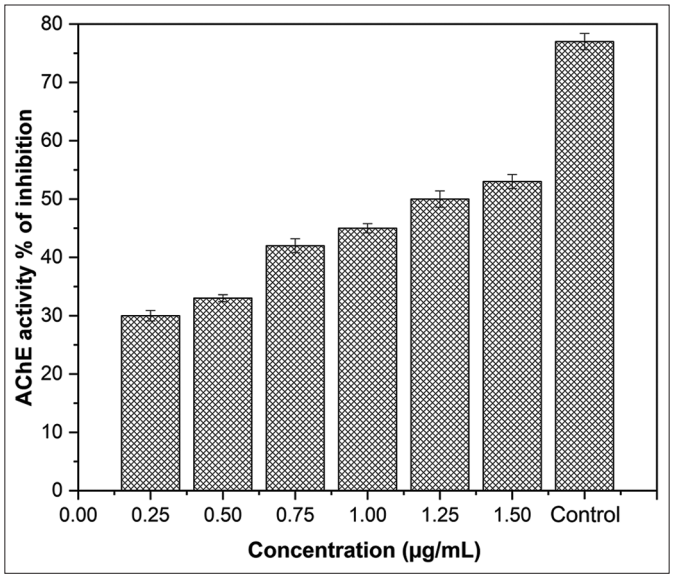

Figure 9: Acetylcholinesterase inhibitory activity of catechin-coated zinc oxide nanoparticles's.

Data of the autographic assay for catechin, ZnONPs, and CAT-ZnONPs are shown: The Retention factor (Rf) was determined by TLC for the catechin's observed in 0.63, ZnONP's has been observed in 0.58, and CAT-ZnONP's was in 0.61. *Ochtodes secundiramea* therapeutic potential is supported by the moderate AChEI activity and minimal off-target effects of their plant extracts, which were characterized in previous report [35] as moderate inhibitors.

3.8. Acetylcholinesterase (AChE) inhibitory activity

The concentrations of CAT-ZnONPs (0.25, 0.50, 0.75, 1, 1.25, and 1.5 µg/mL) and corresponding percentage inhibition values are shown in [Figure 9]. The *in vitro* analysis of CAT-ZnONPs' AChE inhibition potential was demonstrated in a dose-dependent manner with increasing concentrations of CAT-ZnONPs for its potential to inhibit AChE activity given as Supplementary Table 2. The minimum percentage of AChE inhibition activity was observed at a low concentration of CAT-ZnONPs (0.75 µg/mL). The high concentration of CAT-ZnONPs 1.5 µg/mL showed the maximum percentage of AChE inhibition activity. About 50% of AChE inhibition activity has been found in 1.25 µg/mL of the CAT-ZnONPs, so the IC_{50} dosage of nanoparticles with a concentration of 1.25 µg/mL was demonstrated.

In a related investigation, *Withania somnifera* lowered AChE activity by 30% when used at a concentration of 12.50 µg/mL, and reached roughly 50% inhibition at 50 µg/mL [36]. A previous study in oral treatment of ZnONPS and ZnCAP for brain abnormalities caused by retinone RTNE has significantly higher inhibition activity of AChE [37]. Previously reported, the highest AChE inhibitory activity (IC_{50} = 336.885.52 µg/mL) was observed in methanol extract of pericarp; additionally, green tea and tea polyphenols have potentially inhibited AChE with IC_{50} concentration of 30 µg/mL and 248 µg/mL, respectively [21].

4. CONCLUSION

Camellia sinensis was used to biosynthesize CAT-ZnONPs. The outcomes of the CAT-ZnONPs characterization examination using UV-VIS, FTIR, FE-SEM, EDAX, and XRD demonstrate that the material fits the criteria for an excellent nanodrug. The potential for the CAT-ZnONPs' high AChE inhibitory activity was there. *In vitro* studies of CAT-ZnONPs could be conducted in the future, as they have been shown to be an effective medicine for treating neuroprotective effects *in vivo*.

5. ACKNOWLEDGMENTS

The author thankful to Avinashilingam Institute for Home Science and Higher Education for Women, University, Coimbatore, for providing adequate help required to carry out the work.

6. AUTHORS' CONTRIBUTIONS

All authors made substantial contributions to conception and design, acquisition of data, or analysis and interpretation of data; took part in drafting the article or revising it critically for important intellectual content; agreed to submit to the current journal; gave final approval of the version to be published; and agreed to be accountable for all aspects of the work. All the authors are eligible to be an author as per the International Committee of Medical Journal Editors (ICMJE) requirements/guidelines.

7. FUNDING

There is no funding to report.

8. CONFLICTS OF INTEREST

The authors report no financial or any other conflicts of interest in this work.

9. ETHICAL APPROVALS

This study does not involve experiments on animal or human subjects.

10. DATA AVAILABILITY

The data that are supporting the findings of the study are available within the article.

11. PUBLISHER'S NOTE

This journal remains neutral with regard to jurisdictional claims in published institutional affiliation.

REFERENCES

1. Huang C, Notten A, Rasters N. Nanoscience and technology publications and patents: A review of social science studies and search strategies. J Technol Transfer 2011;36:145-72.
2. Mehmandoust M, Erk N, Karaman O, Karimi F, Bijad M, Karaman C. Three-dimensional porous reduced graphene oxide decorated with carbon quantum dots and platinum nanoparticles for highly selective determination of azo dye compound tartrazine. Food Chem Toxicol 2021;158:112698.
3. Karimi-Maleh H, Beitollahi H, Kumar PS, Tajik S, Jahani PM, Karimi F, *et al*. Recent advances in carbon nanomaterials-based electrochemical sensors for food azo dyes detection. Food Chem Toxicol 2022;164:112961.
4. Ashrafizadeh M, Aghamiri S, Tan SC, Zarrabi A, Sharifi E, Rabiee N, *et al*. Nanotechnological approaches in prostate cancer therapy: Integration of engineering and biology. Nano Today 2022;45:101532.
5. Cheraghi S, Taher MA, Karimi-Maleh H, Karimi F, Shabani-Nooshabadi M, Alizadeh M, *et al*. Novel enzymatic graphene oxide

based biosensor for the detection of glutathione in biological body fluids. Chemosphere 2022;287:132187.
6. Orooji Y, Tanhaei B, Ayati A, Tabrizi SH, Alizadeh M, Bamoharram FF, *et al*. Heterogeneous UV-switchable Au nanoparticles decorated tungstophosphoric acid/TiO2 for efficient photocatalytic degradation process. Chemosphere 2021;281:130795.
7. Karimi F, Ayati A, Tanhaei B, Sanati AL, Afshar S, Kardan A, *et al*. Removal of metal ions using a new magnetic chitosan nano-bio-adsorbent; A powerful approach in water treatment. Environ Res 2022;203:111753.
8. Hojjati-Najafabadi A, Mansoorianfar M, Liang T, Shahin K, Karimi-Maleh H. A review on magnetic sensors for monitoring of hazardous pollutants in water resources. Sci Total Environ 2022;824:153844.
9. Fouda A, Abdel-Maksoud G, Abdel-Rahman MA, Salem SS, Hassan SE, El-Sadany MA. Eco-friendly approach utilizing green synthesized nanoparticles for paper conservation against microbes involved in biodeterioration of archaeological manuscript. Int Biodeterior Biodegradation 2019;142:160-9.
10. Alsharif SM, Salem SS, Abdel-Rahman MA, Fouda A, Eid AM, Hassan SE, *et al*. Multifunctional properties of spherical silver nanoparticles fabricated by different microbial taxa. Heliyon 2020;6:e03943.
11. Aref MS, Salem SS. Bio-callus synthesis of silver nanoparticles, characterization, and antibacterial activities via *Cinnamomum camphora* callus culture. Biocatal Agric Biotechnol 2020;27:101689.
12. Herlekar M, Barve S, Kumar R. Plant-mediated green synthesis of iron nanoparticles. J Nanopart 2014;2014:140614.
13. Salem SS, El-Belely EF, Niedbała G, Alnoman MM, Hassan SE, Eid AM, *et al*. Bactericidal and *in-vitro* cytotoxic efficacy of silver nanoparticles (Ag-NPs) fabricated by endophytic actinomycetes and their use as coating for the textile fabrics. Nanomaterials 2020;10:2082.
14. Waris A, Din M, Ali A, Ali M, Afridi S, Baset A, *et al*. A comprehensive review of green synthesis of copper oxide nanoparticles and their diverse biomedical applications. Inorg Chem Commun 2021;123:108369.
15. Kumar H, Bhardwaj K, Kuča K, Kalia A, Nepovimova E, Verma R, *et al*. Flower-based green synthesis of metallic nanoparticles: Applications beyond fragrance. Nanomaterials (Basel) 2020;10:766.
16. Calixto GM, Bernegossi J, De Freitas LM, Fontana CR, Chorilli M. Nanotechnology-based drug delivery systems for photodynamic therapy of cancer: A review. Molecules 2016;21:342.
17. Jan H, Shah M, Andleeb A, Faisal S, Khattak A, Rizwan M, *et al*. Plant-based synthesis of zinc oxide nanoparticles (ZnO-NPs) using aqueous leaf extract of *Aquilegia pubiflora*: Their antiproliferative activity against HepG2 cells inducing reactive oxygen species and other *in vitro* properties. Oxid Med Cell Longev 2021;2021:4786227.
18. Preedy VR, editor. Processing and Impact on Antioxidants in Beverages. Netherlands: Elsevier; 2014.
19. Chan EW, Lim YY, Chew YL. Antioxidant activity of *Camellia sinensis* leaves and tea from a lowland plantation in Malaysia. Food Chem 2007;102:1214-22.
20. Henning SM, Niu Y, Lee NH, Thames GD, Minutti RR, Wang H, *et al*. Bioavailability and antioxidant activity of tea flavanols after consumption of green tea, black tea, or a green tea extract supplement. Am J Clin Nutr 2004;80:1558-64.
21. Jo YH, Yuk HG, Lee JH, Kim JC, Kim R, Lee SC. Antioxidant, tyrosinase inhibitory, and acetylcholinesterase inhibitory activities of green tea (*Camellia sinensis L*.) seed and its pericarp. Food Sci Biotechnol 2012;21:761-8.
22. Okello EJ, Leylabi R, McDougall GJ. Inhibition of acetylcholinesterase by green and white tea and their simulated intestinal metabolites. Food Funct 2012;3:651-61.
23. Ajayan AS, Hebsur NB. Green synthesis of zinc oxide nanoparticles using tea (*Camellia sinesis*) and *Datura* (*Datura stramonium*) leaf extract and their characterization. Chem Sci Rev Lett 2021;10:150-7.
24. Gnanasangeetha D, Thambavani SD. Facile and eco-friendly method for the synthesis of zinc oxide nanoparticles using *Azadirachta* and *Emblica*. Int J Pharm Sci Res 2014;5:2866.
25. Arasoğlu T, Derman S, Mansuroğlu B, Uzunoğlu D, Koçyiğit B, Gümüş B, *et al*. Preparation, characterization, and enhanced antimicrobial activity: Quercetin-loaded PLGA nanoparticles against foodborne pathogens. Turk J Biol 2017;41:127-40.
26. Liu B, Wang Y, Yu Q, Li D, Li F. Synthesis, characterization of catechin-loaded folate-conjugated chitosan nanoparticles and their anti-proliferative effect. CyTA J Food 2018;16:868-76.
27. Rahman MM, Islam MB, Biswas M, Alam AH. *In vitro* antioxidant and free radical scavenging activity of different parts of *Tabebuia pallida* growing in Bangladesh. BMC Res Notes 2015;8:621.
28. Najafabad AM, Jamei R. Free radical scavenging capacity and antioxidant activity of methanolic and ethanolic extracts of plum (*Prunus domestica L*.) in both fresh and dried samples. Avicenna J Phytomed 2014;4:343-53.
29. Rhee IK, van de Meent M, Ingkaninan K, Verpoorte R. Screening for acetylcholinesterase inhibitors from *Amaryllidaceae* using silica gel thin-layer chromatography in combination with bioactivity staining. J Chromatogr A 2001;915:217-23.
30. Okpara EC, Fayemi OE, Sherif ES, Junaedi H, Ebenso EE. Green wastes mediated zinc oxide nanoparticles: Synthesis, characterization and electrochemical studies. Materials (Basel) 2020;13:4241.
31. Arasoglu T, Derman S, Mansuroglu B. Comparative evaluation of antibacterial activity of caffeic acid phenethyl ester and PLGA nanoparticle formulation by different methods. Nanotechnology 2015;27:025103.
32. Al Abdullah K, Awad S, Zaraket J, Salame C. Synthesis of ZnO nanopowders by using Sol-Gel and studying their structural and electrical properties at different temperature. Energy Procedia 2017;119:565-70.
33. Zhang J, Zhou X, Yu Q, Yang L, Sun D, Zhou Y, *et al*. Epigallocatechin-3-gallate (EGCG)-stabilized selenium nanoparticles coated with Tet-1 peptide to reduce amyloid-β aggregation and cytotoxicity. ACS Appl Mater Interfaces 2014;6:8475-87.
34. Mathew A, Fukuda T, Nagaoka Y, Hasumura T, Morimoto H, Yoshida Y, *et al*. Curcumin loaded-PLGA nanoparticles conjugated with Tet-1 peptide for potential use in Alzheimer's disease. PLoS One 2012;7:e32616.
35. Machado LP, Carvalho LR, Young MC, Cardoso-Lopes EM, Centeno DC, Zambotti-Villela L, *et al*. Evaluation of acetylcholinesterase inhibitory activity of Brazilian *red* macroalgae organic extracts. Rev Bras Farmacogn 2015;25:657-62.
36. Khan MA, Srivastava V, Kabir M, Samal M, Insaf A, Ibrahim M, *et al*. Development of synergy-based combination for learning and memory using *in vitro*, *in vivo* and TLC-MS-bioautographic studies. Front Pharmacol 2021;12:678611.
37. Akintunde JK, Farai TI, Arogundade MR, Adeleke JT. Biogenic zinc-oxide nanoparticles of *Moringa oleifera* leaves abrogates rotenone induced neuroendocrine toxicity by regulation of oxidative stress and acetylcholinesterase activity. Biochem Biophys Rep 2021;26:100999.

How to cite this article:
Baskaran N, Subash A. *In vitro* antioxidant and acetylcholinesterase activities of catechin-loaded green fabricated zinc oxide nanoparticles. J App Biol Biotech. 2023;11(6):178-184. DOI: 10.7324/JABB.2023.131095

SUPPLEMENTARY MATERIALS

Supplementary Table 1: DPPH radical scavenging activity.

S. No.	CAT-ZnONPs		Ascorbic acid	
	Concentration (µg/mL)	% of scavenging	Concentration (µg/mL)	% of scavenging
1.	25	40	25	52
2.	30	42	30	60
3.	35	50	35	63
4.	40	58	40	65
5.	45	68	45	72

CAT-ZnONPs: Catechin-coated zinc oxide nanoparticles

Supplementary Table 2: AChE inhibition activities.

S. No.	CAT-ZnONPs	
	Concentration (µg/mL)	% of AChE inhibition
1.	0.25	30
2.	0.5	33
3.	0.75	42
4.	1	45
5.	1.25	50
6.	1.5	53
7.	1.75	77

AChE: Acetylcholinesterase, CAT-ZnONPs: Catechin-coated zinc oxide nanoparticles